Redox Biology 51 (2022) 102266

Contents lists available at ScienceDirect

Redox Biology

journal homepage: www.elsevier.com/locate/redox

Inorganic nitrate and nitrite ameliorate kidney fibrosis by restoring lipid metabolism via dual regulation of AMP-activated protein kinase and the AKT-PGC1α pathway

Xuechen Li [a,b], Zhengbing Zhuge [b], Lucas Rannier R.A. Carvalho [b], Valdir A. Braga [c], Ricardo Barbosa Lucena [d], Shuijie Li [e], Tomas A. Schiffer [b], Huirong Han [b], Eddie Weitzberg [b,f], Jon O. Lundberg [b], Mattias Carlström [b,*]

[a] Beijing Key Laboratory of New Drug Mechanisms and Pharmacological Evaluation Study, Institute of Materia Medica, Chinese Academy of Medical Science & Peking Union Medical College, Beijing, China
[b] Department of Physiology and Pharmacology, Karolinska Institutet, Stockholm, Sweden
[c] Department of Biotechnology, Federal University of Paraíba, João Pessoa, PB, Brazil
[d] Department of Veterinary Sciences, Federal University of Paraíba, Areia, PB, Brazil
[e] Department of Microbiology and Tumor and Cell Biology, Karolinska Institutet, Stockholm, Sweden
[f] Department of Perioperative Medicine and Intensive Care, Karolinska University Hospital, Stockholm, Sweden

ARTICLE INFO

Keywords:
Inorganic nitrate
Nitrite
Renal fibrosis
Oxidative stress
AMPK
PGC1α

ABSTRACT

Background: Renal fibrosis, associated with oxidative stress and nitric oxide (NO) deficiency, contributes to the development of chronic kidney disease and renal failure. As major energy source in maintaining renal physiological functions, tubular epithelial cells with decreased fatty acid oxidation play a key role in renal fibrosis development. Inorganic nitrate, found in high levels in certain vegetables, can increase the formation and signaling by bioactive nitrogen species, including NO, and dampen oxidative stress. In this study, we evaluated the therapeutic value of inorganic nitrate treatment on development of kidney fibrosis and investigated underlying mechanisms including regulation of lipid metabolism in tubular epithelial cells.

Methods: Inorganic nitrate was supplemented in a mouse model of complete unilateral ureteral obstruction (UUO)-induced fibrosis. Inorganic nitrite was applied in transforming growth factor β-induced pro-fibrotic cells *in vitro*. Metformin was administrated as a positive control. Fibrosis, oxidative stress and lipid metabolism were evaluated.

Results: Nitrate treatment boosted the nitrate-nitrite-NO pathway, which ameliorated UUO-induced renal dysfunction and fibrosis in mice, represented by improved glomerular filtration and morphological structure and decreased renal collagen deposition, pro-fibrotic marker expression, and inflammation. In human proximal tubule epithelial cells (HK-2), inorganic nitrite treatment prevented transforming growth factor β-induced pro-fibrotic changes. Mechanistically, boosting the nitrate-nitrite-NO pathway promoted AMP-activated protein kinase (AMPK) phosphorylation, improved AKT-mediated peroxisome proliferator-activated receptor-γ coactivator 1-α (PGC1α) activity and restored mitochondrial function. Accordingly, treatment with nitrate (*in vivo)* or nitrite (*in vitro)* decreased lipid accumulation, which was associated with dampened NADPH oxidase activity and mitochondria-derived oxidative stress.

Conclusions: Our findings indicate that inorganic nitrate and nitrite treatment attenuates the development of kidney fibrosis by targeting oxidative stress and lipid metabolism. Underlying mechanisms include modulation of AMPK and AKT-PGC1α pathways.

Abbreviations: AMPK, AMP-activated protein kinase; PGC-1α, Peroxisome proliferator-activated receptor-γ coactivator 1-α.

* Corresponding author. Department of Physiology and Pharmacology, Karolinska Institutet, Solnavägen 9, Biomedicum 5B, 17177, Stockholm, Sweden.
E-mail address: mattias.carlstrom@ki.se (M. Carlström).

https://doi.org/10.1016/j.redox.2022.102266
Received 11 January 2022; Accepted 9 February 2022
Available online 17 February 2022

1. Introduction

Renal fibrosis is closely associated with progressive chronic kidney disease, which is linked with inflammation and oxidative stress [1,2]. Emerging evidence has demonstrated a link between energy metabolism, especially lipid metabolism and development of renal fibrosis [3,4]. As an energy source of maintaining physiological functioning in the kidney, proximal tubular epithelial cells (TECs) primarily utilize fatty acid oxidation to generate ATP. Decreased fatty acid oxidation in TECs leads to decreased ATP production, lipid deposition, and development of renal fibrosis [5]. Mechanistically, progressive fibrosis is coupled with reduced Acetyl CoA carboxylase (ACC) phosphorylation, compromised fatty acid oxidation and increased lipid accumulation [6].

Inorganic nitrate is naturally found in our diet with particular high levels in leafy greens and in beetroot [7]. This anion is converted to nitrite by oral bacteria and thereafter reduced to bioactive nitrogen species including nitric oxide (NO) in blood and tissues [8]. Dietary boosting of this nitrate-nitrite-NO pathway has been shown to increase NO bioactivity or signaling (cGMP dependent or independent mechanisms) in several experimental models of cardiovascular, renal and metabolic disease [9–11]. Favorable effects associated with nitrate/nitrite treatment include reduction of lipid accumulation, inflammation and fibrosis, which mechanistically have been coupled to reduction of oxidative stress and activation of AMP-activated protein kinase (AMPK) signaling (for review see Ref. [12]).

In this study, we investigated the hypothesis that treatment with inorganic nitrate may have therapeutic value in a model of unilateral ureteral obstruction (UUO)-induced fibrosis. Underlying mechanisms were further investigated in human proximal tubule epithelial cells (HK-2), focusing on energy and lipid metabolism. The effects of nitrate (*in vivo*) and nitrite (*in vitro*) were compared, head-to-head, with metformin. This antidiabetic drug was previously shown to prevent UUO-induced fibrosis and TGF-β-induced oxidative stress via increased ACC phosphorylation and AMPK activation [6,13], and was therefore used as a positive control in the present study.

2. Materials and methods

2.1. Animals and in vivo experimental procedures

The animal study was approved by Institutional Animal Care and Use Committee in Stockholm. Male C57BL/6J mice (8–10 weeks of age) were purchased from Janvier Labs, housed in a temperature and humidity-controlled environment with free access to food and drinking water. The mice were acclimatized during a 7-day period prior to the experiment, meanwhile trained in the tail-cuff system for blood pressure measurement and in the metabolic cages for urine collection. Then, they were randomly allocated to Sham group (n = 8), UUO group (n = 9), UUO + nitrate group (n = 10) and UUO + metformin group (n = 9). Sodium chloride (10 mM, Sigma-Aldrich, #31434), sodium nitrate (10 mM, Sigma-Aldrich, #S5506) or metformin (0.4 mg/ml, Sigma-Aldrich, #D150959) was administrated in drinking water five days before the UUO surgery, until the mice were sacrificed. Since dietary nitrate supplementation in healthy control animals has not been associated with any major cardiometabolic effects [9–11], these treatment arms in sham-operated control groups were not included in this study.

2.1.1. Unilateral ureteral obstruction

UUO surgery was performed after the mice were anesthetized by inhalation of 2.2% isoflurane (Abbott Scandinavia AB) in air (flow rate of 200 ml/min). The mice undergoing surgery were all confirmed to be deeply anesthetized throughout the operation. The left ureter was completely ligated using the 6-0 non-absorbable silk suture (AgnThos, #681H). Sham group mice were proceeded to the same operation without left ureter ligation.

2.1.2. Tail-cuff blood pressure monitoring

Three days after the surgery, conscious blood pressure (systolic, diastolic and mean arterial pressure) was monitored using Coda High Throughput Noninvasive Tail Monitoring System (Kent Scientific, Torrington, CT, USA), following the manufacturer's protocol. Only collected data that was validated and accepted by the Manufactor's software program were included for further analysis.

2.1.3. Metabolic cages and euthanization

Following completed blood pressure monitoring, the mice were transferred to the metabolic cage (Tecniplast) for 24 h and the 24-hour urine was collected together with a single blood sample from the tail. Six days after the surgery, all mice were euthanized under isoflurane anesthesia (described above). Kidney tissues and blood from inferior vena cava were collected for further analyses.

2.2. Plasma nitrate, nitrite and cGMP measurement

Blood was collected into tubes containing EDTA (Sigma-Aldrich, #E9884), final concentration 2 mM and was immediately centrifuged at 4700 × *g* for 5 min to obtain plasma fraction. Plasma nitrate and nitrite were analyzed using HPLC (ENO-20) as described in detail previously [12]. To prevent degradation of cGMP, the plasma was transferred to tubes containing a PDE inhibitor, IBMX (3-Isobutyl-1methylxanthine; Sigma-Aldrich, #I5879) to give a final concentration 10 μM. Samples were thereafter frozen and stored at −80 °C, before analyzed for cGMP. The measurement was done by using an ELISA kit (GE Healthcare, #RPN226), according to the manufacturers' instructions. All absorbance reading was done in SpextraMax iD3 (Molecular Devices).

2.3. Determination of creatinine clearance

The 24-hour urine was collected from the metabolic cages. Creatinine levels in plasma and urine were measured by using ELISA kit from Cayman Chemical #700460 or #500701, respectively, according to the manufacturers' instructions. The creatinine clearance was thereafter calculated to estimate glomerular filtration rate. *i.e.* creatinine clearance = urine creatinine concentration × 24hour urine output volume/plasma creatinine concentration.

2.4. Vascular reactivity

Isolated renal interlobular arteries were mounted in myograph chambers (Danish Myo Technology, model 620 M) filled with oxygenated Krebs buffer. Vascular reactivity was evaluated as described previously [12]. In brief, each vessel underwent a normalization procedure to set the resting tension, and the viability was assessed by the responses to 0.1 M potassium chloride. Dose-dependent vascular responses to phenylephrine or acetylcholine were evaluated.

2.5. Histopathology examination

Paraformaldehyde-fixed kidneys (approx. 24h fixation) were dehydrated in increasing concentrations of ethanol, diaffinized by xylol and embedded in liquid paraffin. The kidney tissue blocks were cut by microtome to a thickness of 3 μm. Then, hematoxylin-eosin (HE), Periodic acid-Schiff (PAS) and Masson's Trichrome (MT) stains were performed for evaluation under light microscopy. Slides were evaluated by a blinded histopathologist who examined at least 10 fields at different magnifications. Pathological changes were scored semiquantitatively according to their extent and classified as: Score 0: no pathological changes; Score 1: <10% of the affected area; Score 2: 10–25% of the affected area; Score 3: 25–50% of the affected area; Score 4: 50–74% of the affected area; Score 5: >75% of the affected area [14].

2.6. Triglyceride assay

Kidney triglyceride levels were measured by using a colorimetric kit (Cayman Chemical, #10010303) according to the manufacturer's protocol.

2.7. Cell culture

The human proximal tubular epithelial cell line HK-2 was purchased from ATCC. HK-2 cells were cultured in DMEM/F12 medium (Thermo Fisher Scientific) containing 10% FBS (Gibco), 0.05 mg/ml BPE (Thermo Fisher Scientific), 5 ng/ml EGF (Thermo Fisher Scientific), 100 U/ml penicillin and streptomycin (Thermo Fisher Scientific) in a 37 °C incubator with 5% CO_2. For cell experiments, HK-2 cells were pretreated by 10 μM sodium nitrite (Sigma-Aldrich, S2252), or 100 μM metformin, or 1 μM AKT inhibitor VIII (Calbiochem, #124018) for 30 min, followed by 50 ng/ml transforming growth factor beta (TGFβ, Sigma-Aldrich, #T7039) induction for 24 h or 48 h. Cells were subsequently harvested for further measurements.

2.8. Western blot

Kidney tissues or cells were lysed with ice-cold RIPA buffer (1% sodium deoxycholate, 1% Triton X-100, 20% SDS, 0.15 M sodium chloride, 1 mM EDTA pH 8.0, 10 mM Tris-HCl pH 7.5). Protease inhibitor (1:1000; Sigma-Aldrich) and phosphatase inhibitor (1:100; Sigma-Aldrich) were added to prevent degradation. After ultrasonication, the lysates were centrifuged at 12000 × *g* for 10 min. Protein level was assessed using the BCA assay (Bio-Rad). Equal amount of protein samples was subjected for SDS-PAGE separation followed by transferring to PVDF membranes. The membranes were blocked using 5% milk for 1 h, and incubated with primary antibodies at 4 °C overnight. Primary antibodies included anti-fibronectin (Abcam, #ab23750), anti-alpha-smooth muscle actin (α-SMA, Cell Signaling Technology, #19245S), *anti*-vinculin (Santa Cruz Biotechnology, #sc25336), *anti*-p-AKT (Cell Signaling Technology, #2965), *anti*-AKT (Cell Signaling Technology, #9272S), *anti*-p-PGC1α (R&D Systems, #AF6650), *anti*-PGC1α (Santa Cruz Biotechnology, #sc13067), *anti*-p-AMPK (Cell Signaling Technology, #2531L), *anti*-AMPK (Cell Signaling Technology, #2532L), *anti*-SREBP (Thermo Fisher Scientific, #MA5-16124), *anti*-p-ACC (Cell Signaling Technology, #3661S), *anti*-NOX2 (BD Biosciences, #611415). Blots were eventually developed using Clarity Western ECL Substrate (Bio-Rad, #170–5061) or SuperSignal West Femto Maximum Sensitivity Substrate (Thermo Fisher Scientific, #34096) in the ChemiDoc Imaging System (Bio-Rad). For Western blots, uncropped, annotated, full-length images with MW markers are shown in Supplemental Fig. S1.

2.9. RT-qPCR

Quantitative reverse-transcription-PCR was performed to assess mRNA expression in kidneys or cells in this study. Kidney tissues or harvested HK-2 cells were homogenized in Trizol reagent (Thermo Fisher Scientific), followed by RNA isolation according to the standard procedure. The RNA concentration and A260/280 ratio were detected using Nanodrop (Thermo Fisher Scientific, #ND-1000). Then 1 μg RNA was reverse transcribed into cDNA using High-capacity cDNA reverse transcription kit (Applied Biosystems, #4368814). qPCR was performed using Power SYBR Green Master Mix (Thermo Fisher Scientific) on the 7500 Real-Time PCR System. Primer sequences are listed in Supplemental Table S1. The data was analyzed using the ΔΔCt-method, standardized to vinculin in kidney samples or GAPDH in cell samples.

2.10. mtDNA/nDNA ratio

HK-2 cell genomic DNA was extracted using PureLink genomic DNA mini kit (Invitrogen, #K182001), according to the manufacturer's instructions. DNA purity and concentration were assessed by Nanodrop. Then 100 ng DNA for each sample was amplified and quantified as mentioned above, using primers of mitochondria-encoded ATP6 and nucleus-encoded GAPDH. Primer sequences are described in Supplemental Table 1. Subsequently the ratio of mitochondrial to nuclear DNA level was calculated.

2.11. Seahorse Mito Stress test

Cells were cultured and treated in the Seahorse XF96 V3 PS microplate (Agilent, #101085-004). The sensor cartridge was hydrated in a non-CO_2 incubator at 37 °C overnight before the assay. On the day of assay, specific assay medium (Seahorse XF DMEM medium with 1 mM sodium pyruvate, 2 mM glutamine and 10 mM glucose, pH 7.4) was replaced to culture the cell for 1 h in a non-CO_2 incubator at 37 °C. Oligomycin, FCCP and antimycin were loaded to the sensor cartridge to reach the final concentration of 1.5 μM, 0.16 μM and 0.5 μM, respectively. The assay was run using the Seahorse XFe96 analyzer (Agilent) according to the manufacturer's protocol. Spare respiratory capacity was calculated as the difference in oxygen consumption rate (OCR) of basal respiration prior to oligomycin treatment and maximum respiration after FCCP treatment.

2.12. NOX activity assay

NADPH oxidase-derived superoxide was measured using a chemiluminescence assay, as introduced previously [12]. In brief, HK-2 cells were collected and re-suspended in 800 μl PBS in the measurement tubes. 5 μM lucigen was added to the cell suspensions in dark for 10 min, then 100 μM NADPH substrate was added to start the reaction. Chemiluminescence signal was detected using AutoLumat multi-tube luminometer (Berthold Technologies, #LB953) every 3 s for 3 min for each sample.

2.13. Determination of mitochondrial superoxide (mitoSOX)

HK-2 cells were seeded and treated in 96-well black/clear bottom plates (Thermo Fisher Scientific). Mitochondrial superoxide (mitoSOX) levels in the cells were measured using a commercial kit (Invitrogen, #M36008) according to the manufacturer's instructions.

2.14. Oil Red O staining

Lipid accumulation was assessed by Oil Red O staining. Cells were fixed with 4% paraformaldehyde for 30 min. After washing with PBS, cells were left air dry for 5 min to avoid clumping stain. ORO solution (3.75 mg/mL) was added to incubate the cells for 1 h. After removing the unstained dye by PBS washing, isopropanol was added to extract the dye within the cells, and the absorbance at 520 nm was measured to quantify the lipid accumulation.

2.15. Statistical analysis

Data are presented as mean ± SEM unless otherwise indicated. Statistical analyses were performed using one-way ANOVA or two-way ANOVA, as appropriated, followed by posthoc test recommended by the software GraphPad Prism 8. Two-way ANOVA analysis followed by Sidak and Tukey multiple comparisons tests were respectively used in vascular reactivity and histopathology evaluation. One-way ANOVA analysis followed by Dunnett's multiple comparisons test was used in the rest experiments. A p value of less than 0.05 was considered statistically significant and indicated in the result section. Statistical trends (*i.e.* P value between 0.05 and 0.09) have also been denoted in the figures. * denotes $P < 0.05$, **$P < 0.01$ and ***$P < 0.001$ between indicated groups.

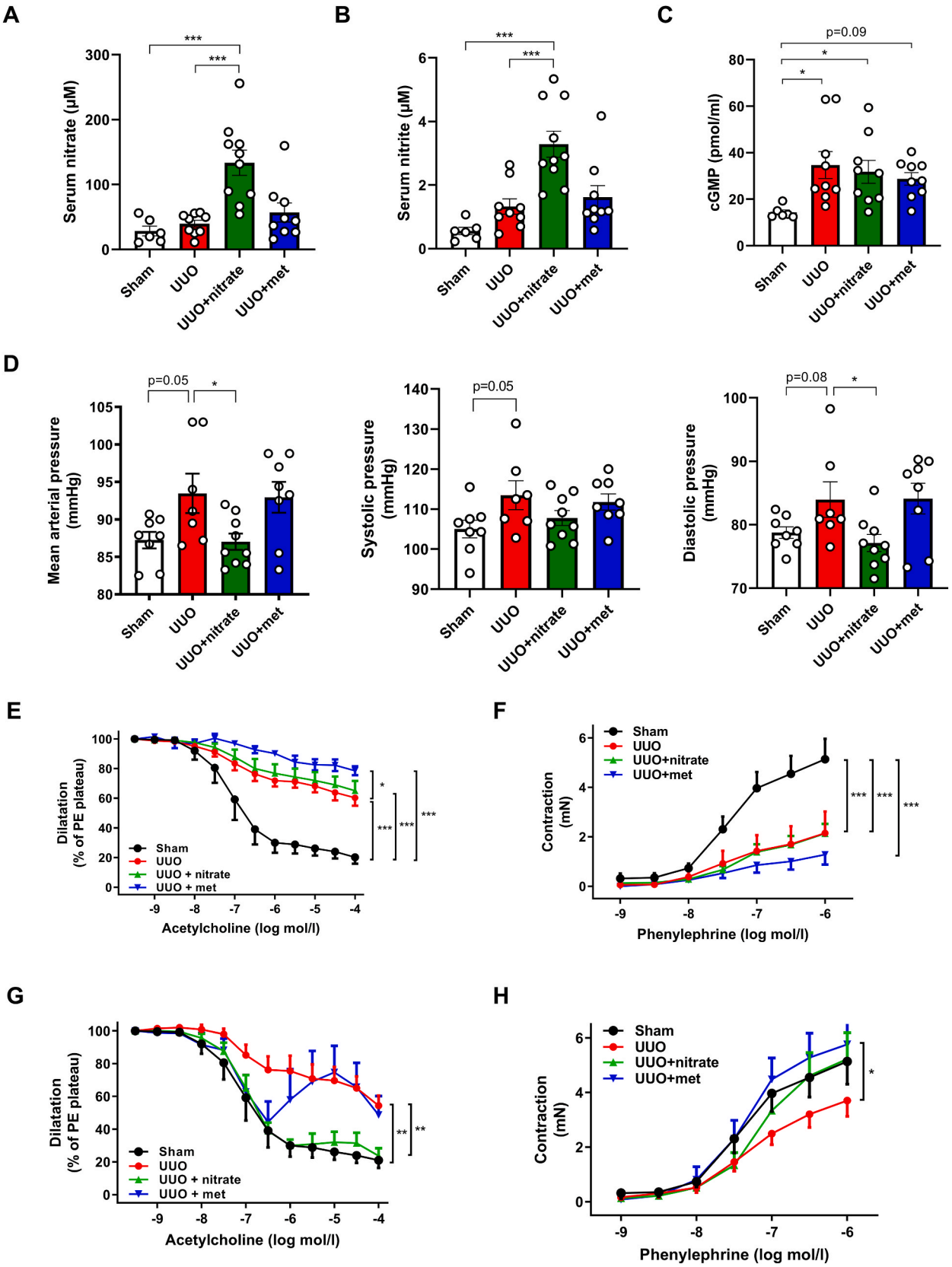

Fig. 1. Nitric oxide homeostasis and cardiovascular characteristics in mice with unilateral ureteral obstruction and effects of nitrate and metformin. Plasma levels of nitrate (A), nitrite (B), cGMP (C) and blood pressure (D). Ex vivo vascular reactivity of interlobular artery from the obstructed left kidney (UUO) (E, F) and the contralateral right kidney (G, H). Data are presented as mean ± SEM. *P < 0.05, ***P < 0.001 between indicated groups.

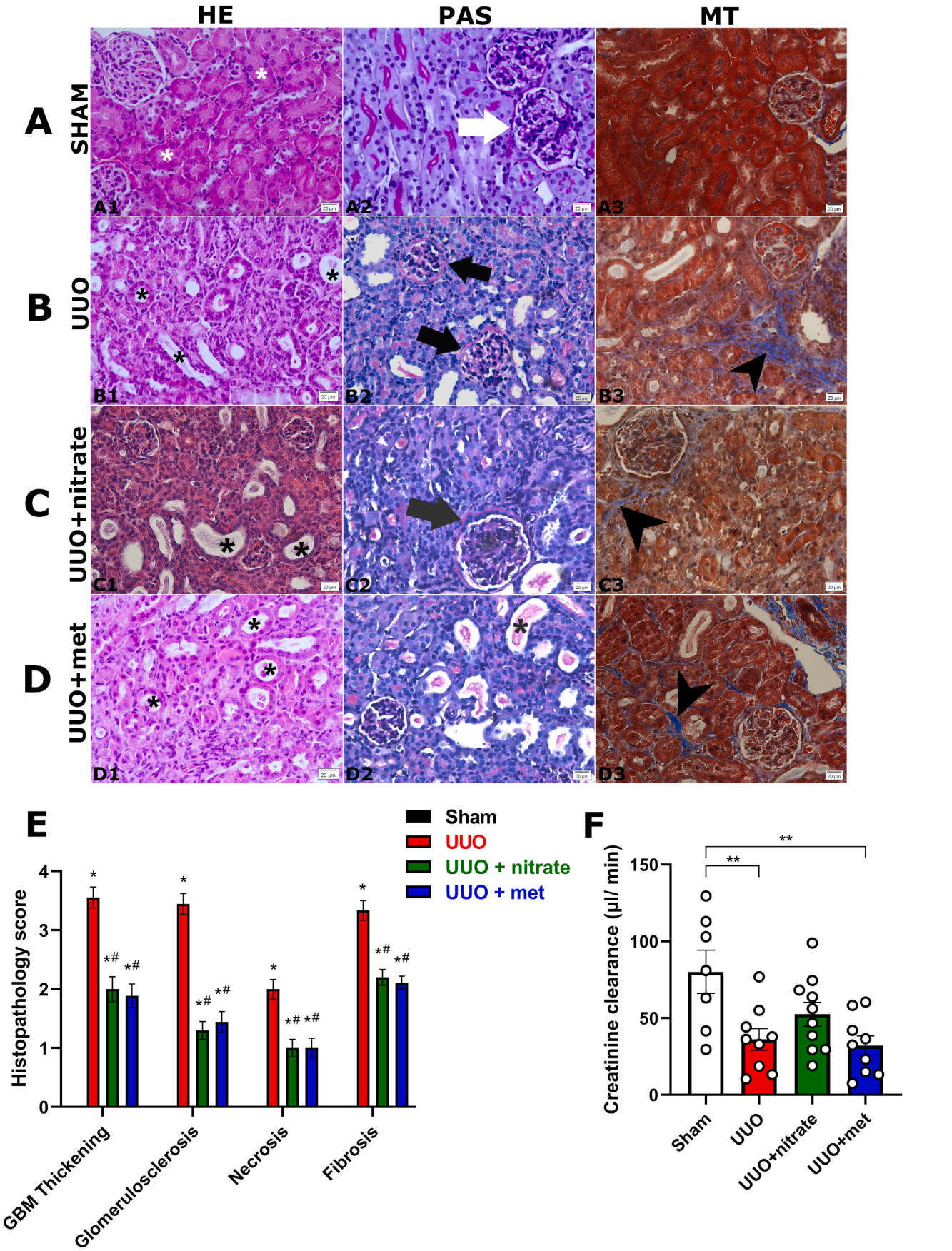

(caption on next page)

Fig. 2. Nitrate ameliorates kidney injury in mice with unilateral ureteral obstruction. Histological kidney sections stained with Hematoxylin and Eosin (HE), Periodic acid-Schiff (PAS) and Masson's Trichrome (MT). Photomicrographs of the left renal cortex from sham-operated mice (A) and mice submitted to unilateral ureteral obstruction (UUO) (B) as well as UUO combined with nitrate (C) or metformin (D) treatment (400x magnification). **(A) Sham:** Normal renal parenchyma showing tubules without atrophy or dilation (A1 - white *), urinary space well preserved and glomerular capsule with normal thickness (A2 – white arrow) and absence of inflammatory cells or fibrosis. **(B) UUO:** Renal parenchyma showing clear thickening of the glomerular capsule and glomerulosclerosis (B2 – black arrows), dilation and tubular necrosis (black *) and interstitial fibrosis (B3 – arrowhead). **(C) UUO + nitrate:** Renal parenchyma exhibiting tubular dilation and necrosis (black *), thickening of the glomerular membrane (C2 – black arrow), besides moderate fibrosis (C3 - arrowhead). **(D) UUO + met:** The kidneys exhibiting dilation and tubular necrosis (black *), moderate thickening of the glomerular membrane and fibrosis (D3 – arrowhead). **(E)** Semiquantitative evaluation (scores) of renal histopathological alterations of the effects of treatment with nitrate and metformin on the model of unilateral ureter obstruction (UUO). * vs Sham; # vs UUO. GBM; glomerular basement membrane. **(F)** creatinine clearance to estimate glomerular filtration rate. met; metformin. Data is expressed as mean ± SEM. *P < 0.05 vs. Sham; **P < 0.01 vs. Sham; #P < 0.05 *vs.* UUO.

3. Results

3.1. PART I: In vivo and Ex vivo effects of nitrate

Sodium chloride, sodium nitrate and metformin were administrated via the drinking water and the daily average intake was monitored and calculated. The intake of sodium chloride, sodium nitrate and metformin *per* mouse was 50.9 ± 1.9, 53.4 ± 10.1, 14.8 ± 1.2 μmol/day during the five-days pretreatment period. Post UUO surgery, the intake of sodium chloride, sodium nitrate and metformin was 34.6 ± 5, 38.5 ± 8.2, 9.3 ± 0.7 μmol/day during day 1–3, and 43.2 ± 7.4, 48.8 ± 17, 9.5 ± 1.3 μmol/day during day 4–6 after surgery, respectively.

3.2. Nitrate increases markers of NO signaling and attenuates blood pressure following UUO

Plasma levels of nitrate, nitrite and cGMP increased in UUO mice following nitrate treatment (Fig. 1A–C). Surprisingly, cGMP levels were also elevated in vehicle-treated UUO mice, which might be associated with their cardiovascular phenotype and potentially also activation of inducible NOS (iNOS) associated with their inflammatory profile. Moreover, UUO was associated with elevated blood pressure compared with sham-operated animals, which was completely prevented by nitrate treatment (Fig. 1D). Metformin did not significantly change nitrate or nitrite levels, or blood pressure, which is in agreement with a recent study in mice, demonstrating that nitrate is superior compared with metformin regarding protection against cardiovascular dysfunction [15]. Regarding cGMP we observed a non-significant increase ($p = 0.09$) in metformin treated UUO mice compared with controls.

3.3. Nitrate supplementation modulates vascular reactivity following UUO

Endothelium-dependent vasorelaxation (Fig. 1E) and phenylephrine-induced vasoconstriction (Fig. 1F) in interlobular arteries from the obstructed kidney were impaired following UUO. This was not improved by either nitrate or metformin treatment. An abnormal vascular phenotype was also observed in the contralateral kidney following UUO,

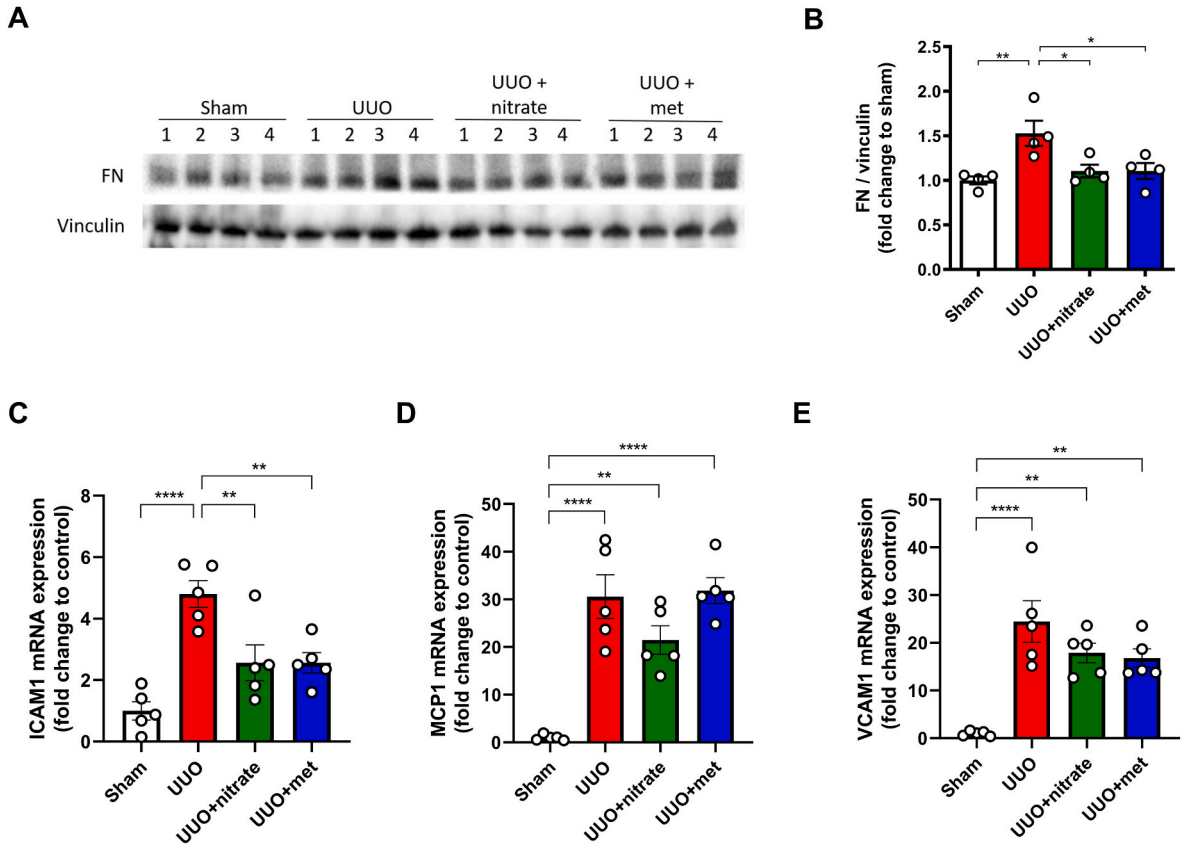

Fig. 3. Nitrate attenuates renal fibrotic and inflammatory changes in mice kidneys with unilateral ureteral obstruction. Fibronectin protein expression in the kidneys with unilateral ureteral obstructioin (UUO) was explored (A) and quantified (B), as well as mRNA expression of ICAM1 (C), MCP1 (D) and VCAM1 (E). Data are presented as mean ± SEM. *P < 0.05, **P < 0.01, ***P < 0.001 between indicated groups.

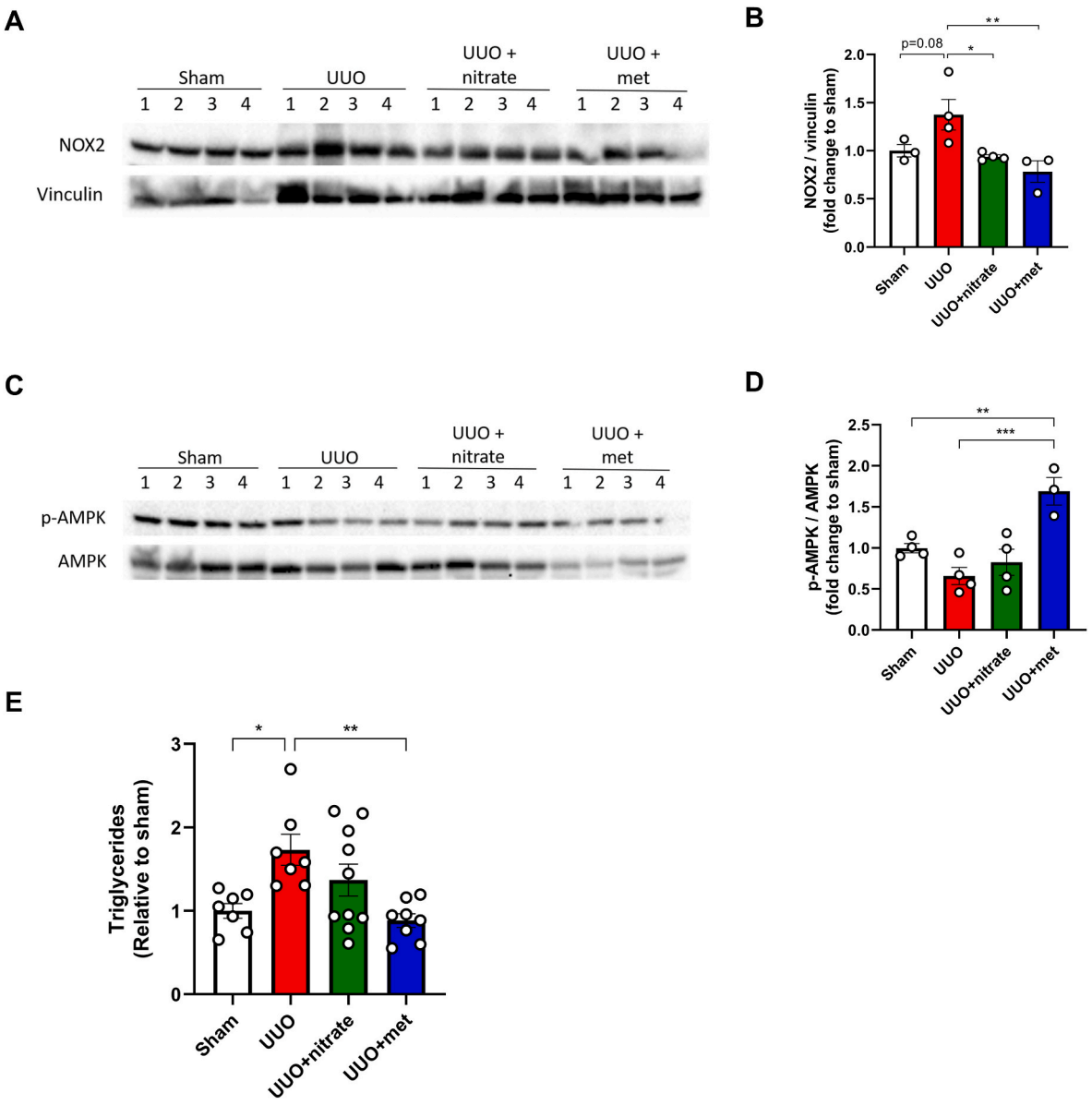

Fig. 4. Nitrate reduces oxidative stress and lipid accumulation in mice kidneys with unilateral ureteral obstruction. Western blot analysis was applied to evaluate the protein expression of NOX2 (A, B), p-AMPK and AMPK (C, D) in the obstructed kidneys (UUO). The triglycerides level in UUO mice kidney was measured (E). UUO; unilateral ureteral obstruction. Data are presented as mean ± SEM. *P < 0.05, **P < 0.01, ***P < 0.001 between indicated groups.

as evident from reduced acetylcholine-mediated vasorelaxation and phenylephrine-induced contraction (Fig. 1G–H). In contrast to that observed in the obstructed kidney, treatment with nitrate prevented the development of endothelium dysfunction in interlobular arteries from the contralateral kidney (Fig. 1G), whereas only partial protection was observed with metformin. Metformin treatment in UUO operated mice was associated with restored vascular contractility (i.e. no difference compared with sham) to phenylephrine in the contralateral kidney, and similar shift in contractility (albeit not statistically significant) was observed with nitrate (Fig. 1H).

3.4. Nitrate dampens renal injuries and glomerular dysfunction as well as fibrotic and inflammatory changes following UUO

UUO was associated with profound renal pathological injuries, as evident from thickening of the capsule and glomerular basement membrane, glomerulosclerosis, tubular atrophy as well as necrotic and fibrotic changes compared with sham-operated animals (Fig. 2A–E). All these renal pathological changes were dampened by nitrate and by metformin. Masson's Trichrome staining of both left and right kidney was shown in Supplementary Fig. S2. Histopathalogical semi-evaluation is presented as individual data in Supplementary Fig. S3. Creatinine clearance was reduced by more than 50% following UUO (Fig. 2F). This reduction in creatinine clearance was less marked in mice with nitrate treatment whereas metformin had no effect. Histopathological signs of fibrosis were supported by increased expression of fibronectin (Fig. 3A–B) and accompanied by inflammatory changes as evident from increased mRNA expression of ICAM1, MCP1 and VCAM1 (Fig. 3C–E).

3.5. Nitrate prevents upregulation of NOX2, impairment of AMPK signaling and accumulation of triglycerides in the kidney following UUO

Expression of NADPH oxidase 2 (NOX2) trended to be increased in the obstructed kidney following UUO (Fig. 4A–B) compared with sham-operated mice (p = 0.08). Treatment with nitrate and metformin significantly reduced NOX2 expression compared with UUO. Moreover,

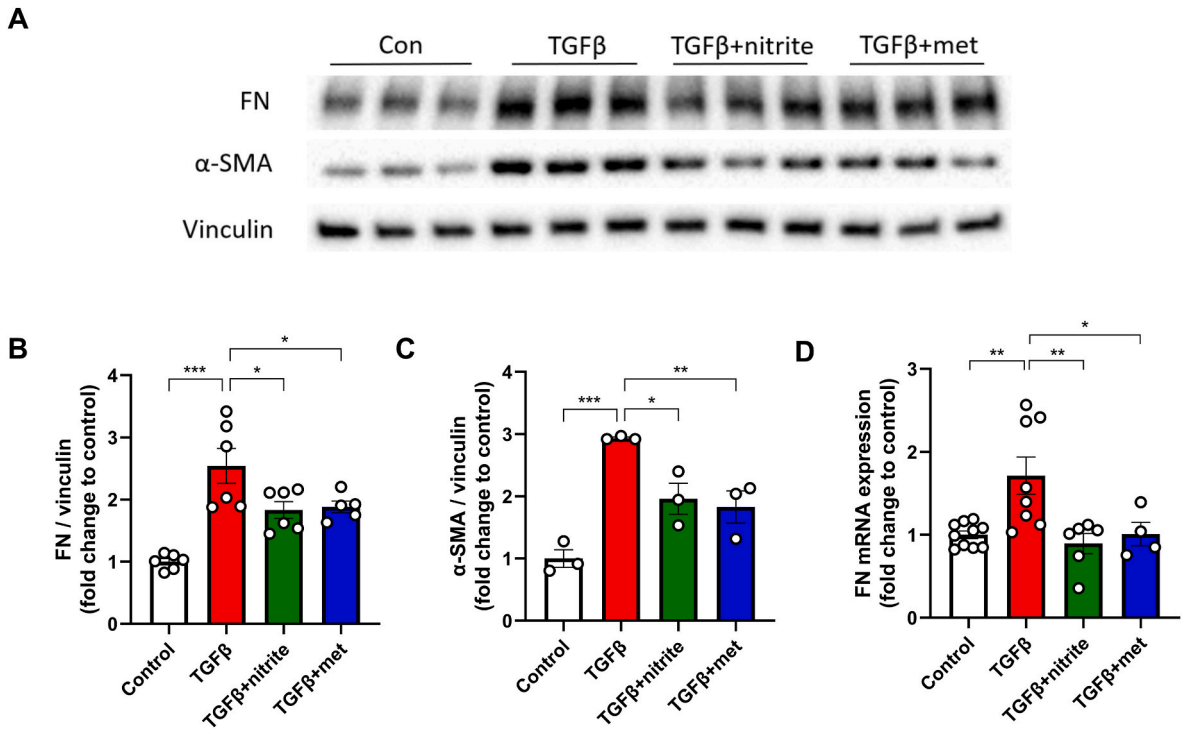

Fig. 5. Nitrite reduces TGFβ-induced fibrosis in HK-2 cells. Tubular cells were induced with 50 ng/ml TGFβ for 48 h, with 10 μM sodium nitrite or 100 μM metformin treatment. Fibronectin and α-SMA protein expression were applied for western blot (A) and followed by quantification (B, C). mRNA expression of fibronectin was evaluated by qPCR (D). Data are presented as mean ± SEM. *P < 0.05, **P < 0.01, ***P < 0.001 between indicated groups.

AMPK activation trended to be reduced and accumulation of triglycerides was increased in obstructed kidney following UUO (Fig. 4C–D). This was prevented by metformin treatment, but not significantly improved by nitrate.

3.6. PART II: In vitro effects of nitrite

In further mechanistic studies, aimed at mimicking the *in vivo* UUO model with renal fibrosis, we used HK-2 cells incubated with TGFβ. In these cell studies we used nitrite instead of nitrate to bypass the first reduction step in the nitrate-nitrite-NO pathway which requires commensal bacteria *in vivo*.

3.7. Nitrite reduces TGFβ-induced fibrosis

Following incubation with TGFβ, fibronectin and α-SMA expression were significantly increased compared with control cells (Fig. 5A–D). Simultaneous treatment with nitrite and metformin dampened TGFβ-induced elevations of both fibronectin and α-SMA.

3.8. Nitrite inhibits NADPH oxidase-derived oxidative stress and lipid accumulation

NADPH oxidase activity was increased following incubation with TGFβ (Fig. 6A), which was accompanied by increased ORO-staining (Fig. 6B). Moreover, incubation with TGFβ decreased AMPK activation and downstream signaling, *i.e.* p-ACC and SREBP expression (Fig. 6C–F). These abnormalities, associated with oxidative stress, lipid accumulation/fibrosis and compromised AMPK signaling, were largely prevented by nitrite or metformin treatment.

3.9. Nitrite dampens TGFβ-induced AKT-mediated PGC1α activation

Cells incubated with TGFβ displayed increased p-AKT and p-PGC1α (S571) expression (Fig. 7A–C). The inhibitory phosphorylation of PGC1α, is associated with decreased PGC1α activity and therefore decreased fatty acid oxidation [16,17]. Treatment with nitrite or metformin (Fig. 7A–C) reduced p-AKT and p-PGC1α expression levels. Treatment with an AKT inhibitor normalized p-AKT levels and trended to reduce TGFβ-induced fibrosis, as indicated by fibronectin expression (Fig. 8A–D), but did not significantly impact on AMPK activation or its downstream ACC signaling (Fig. 8E–G).

3.10. Nitrite improves mitochondrial respiration and dampens production of superoxide

Next, seahorse technique was utilized to assess mitochondrial function. Oxygen consumption rate for all groups is shown in Fig. 9A. Spare respiratory capacity was significantly reduced in cells incubated with TGFβ (Fig. 9B), and this was partially prevented by nitrite treatment while no effect of metformin was observed. Mitochondrial density (calculated as mtDNA/nDNA) was largely unaffected, although the metformin group showed somewhat lower number compared with control cells (Fig. 9C). Production of reactive oxygen species from the mitochondria (*i.e.* mitoSOX) was significantly increased following incubation with TGFβ, and this was prevented by both nitrite and metformin treatment (Fig. 9D).

4. Discussion

In this experimental study, we show that dietary nitrate treatment elevated plasma nitrate and nitrite, reduced blood pressure, and markedly attenuated the development of kidney fibrosis following complete unilateral ureteral obstruction. Mechanistically, boosting the nitrate-nitrite-NO pathway dampened oxidative stress, amplified AMPK signaling, as well as increased PGC1α activity mediated by inactivation of the TGFβ-AKT pathway. Accordingly, downstream fatty acid oxidation was enhanced, and lipid accumulation as well as inflammation was reduced by nitrate/nitrite treatment. In the current study, metformin was used as a positive control to dampen renal fibrosis as this compound

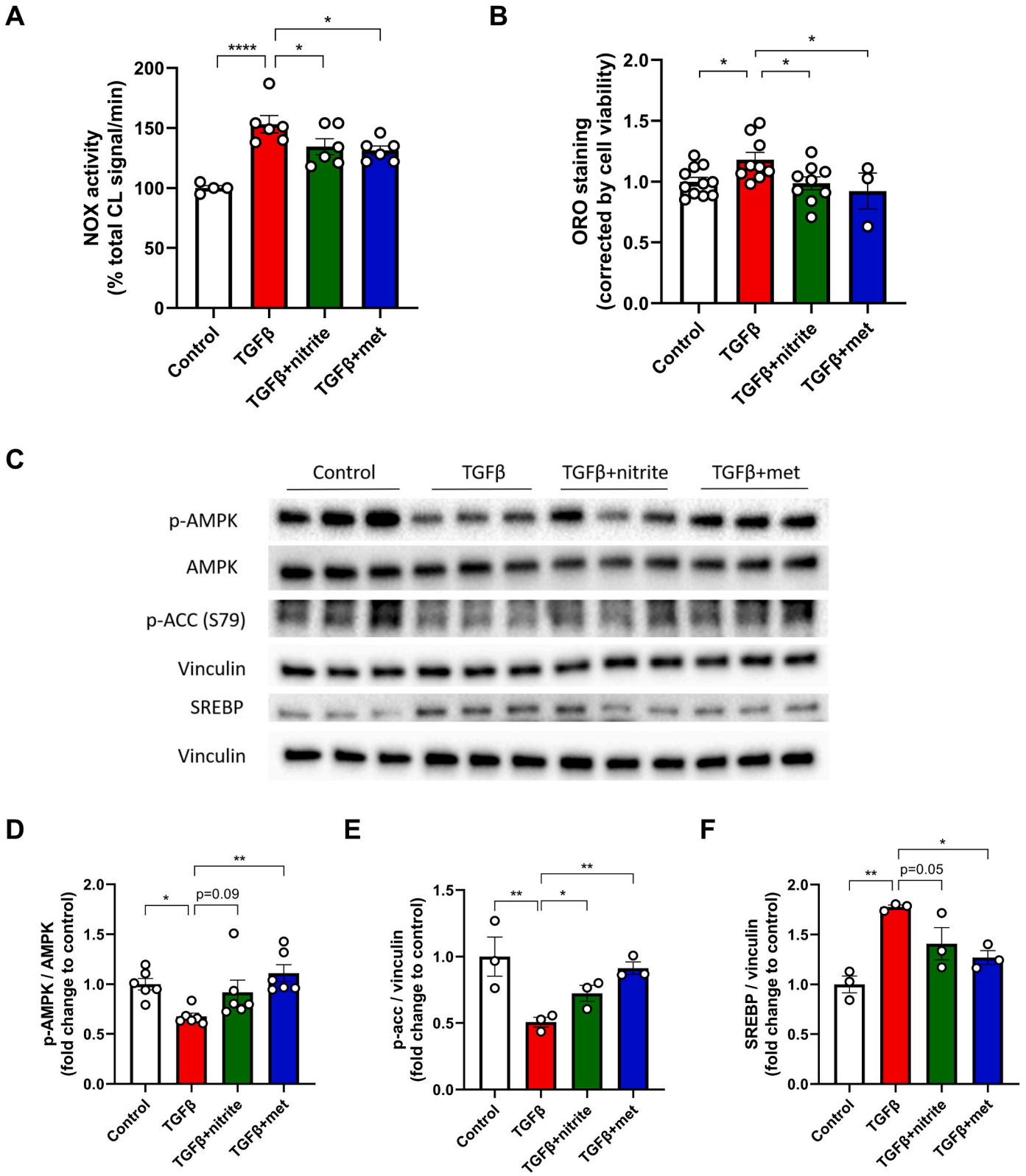

Fig. 6. Nitrite inhibits NADPH oxidase-derived oxidative stress and lipid accumulation. HK-2 cells were induced by 50 ng/ml TGFβ, with 10 μM sodium nitrite or 100 μM metformin treatment. Under 24 h induction, NOX activity was measured (A). Under 48 h induction, oil-red staining was applied to evaluate lipid accumulation (B), and the expression of p-AMPK, AMPK, p-ACC, SREBP were evaluated by western blot (C–F). Data are presented as mean ± SEM. *P < 0.05, **P < 0.01, ***P < 0.001 between indicated groups. (For interpretation of the references to color in this figure legend, the reader is referred to the Web version of this article.)

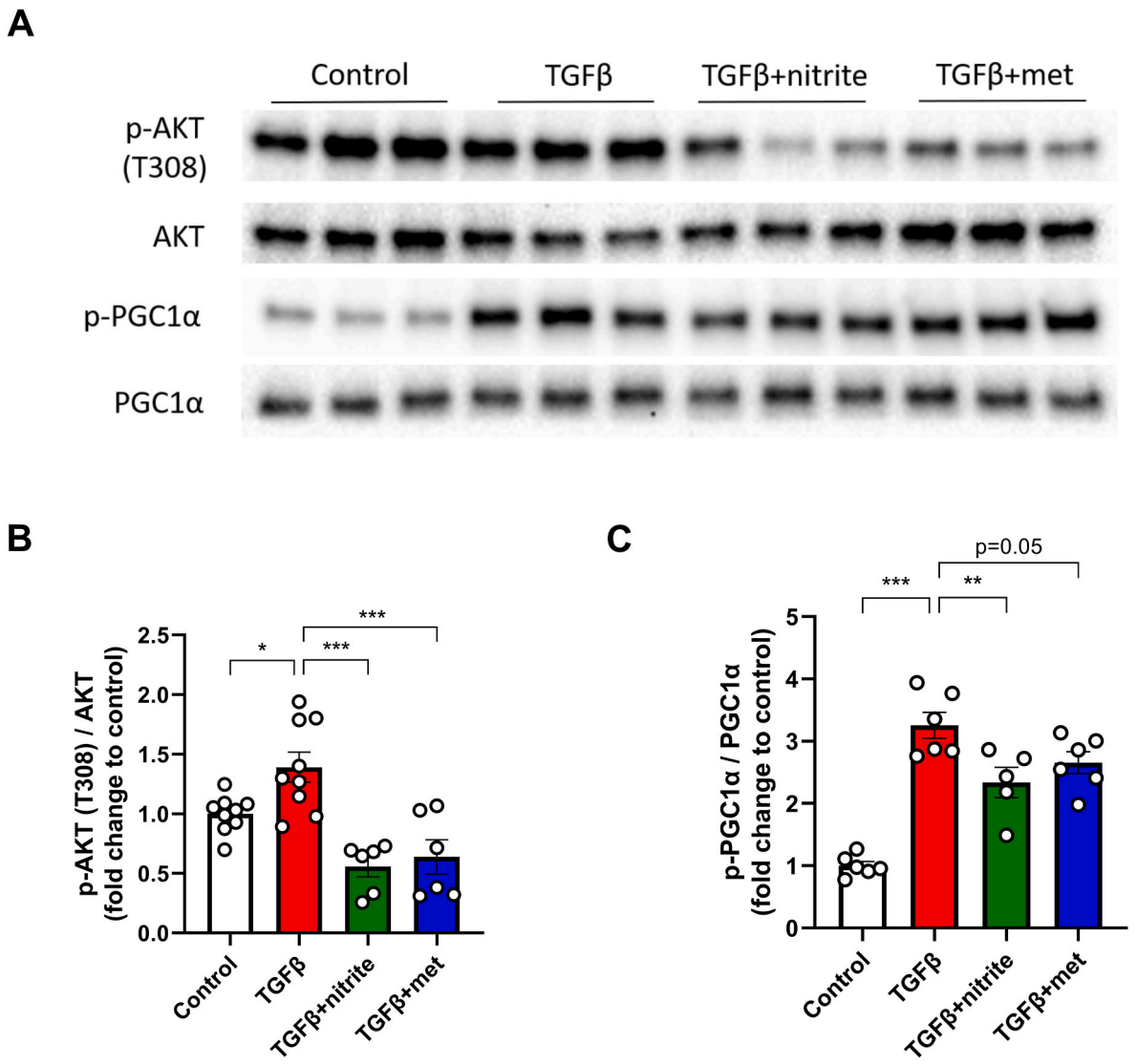

Fig. 7. Nitrite improves AKT-mediated decline in PGC1α activity. HK-2 cells were induced with 50 ng/ml TGFβ for 48 h, with 10 μM sodium nitrite or 100 μM metformin treatment. The protein expression of p-AKT, AKT, p-PGC1α, PGC1α was measured and quantified using western blot (A–C). Data are presented as mean ± SEM. *P < 0.05, **P < 0.01, ***P < 0.001 between indicated groups.

has showed protective effects in this model previously [6]. Our findings suggest that nitrate and nitrite have similar anti-fibrotic effects as metformin *in vivo* and *in vitro*, respectively. Metformin also reduced oxidative stress and preserved PGC1α activity by inhibiting TGFβ-AKT signaling, while showing stronger AMPK and downstream ACC activation than nitrate/nitrite.

Dietary nitrate supplementation has been found to have protective effects in cardiovascular disease [10,18–21]. In this study, nitrate reduced blood pressure, protected against endothelial and glomerular dysfunction in the contralateral kidney, as evident from maintained endothelium-dependent vasorelaxation and better-preserved kidney function. This improvement indicated alleviated burden on the contralateral kidney, which should be of benefit for long-term outcome and potentially even survival. Moreover, several neurohormonal pathways allow for interaction between the two kidneys, in which the contralateral kidney might respond to changes that occur in the ipsilateral kidney [22]. Likely, the protective effects of nitrate on the contralateral kidney could also contribute to benefits of the ipsilateral kidney. In comparison, metformin treatment did not show any significant improvement in cardiovascular function. This is largely in agreement with a previous report [15], which demonstrated that nitrate had similar metabolic effects as metformin but was superior regarding its cardiovascular protection. Of note, in the present study creatinine clearance was used to assess kidney function *in vivo*. This is a limitation since this method has been associated with greater variability and overestimate of glomerular filtration rate due to tubular secretion of creatinine in the mouse [23].

Abnormal lipid metabolism has been associated with kidney disorders [24], and accumulation of lipids was observed in the kidneys of diabetic patients with chronic kidney disease [25]. This has been illustrated as a risk factor for developing renal fibrosis because of lipid toxicity [26]. Defective fatty acid oxidation in tubular epithelial cells has been suggested to play a key role in the development of kidney fibrosis [5]. Correspondingly, we observed accumulated neutral lipids in both the obstructed mouse kidney fibrosis model and in TGFβ-induced pro-fibrosis in human renal tubular cells. Compromised AMPK signaling led to dysregulated fatty acid synthesis and oxidation, and observation supported by increased SREBP and decreased ACC expression downstream of AMPK.

PGC1α which is a master regulator of mitochondria biogenesis, was found less activated following incubation with TGFβ. Accordingly, reduced mitochondrial spare respiratory capacity and excessive mitochondrial superoxide production indicated mitochondrial dysfunction.

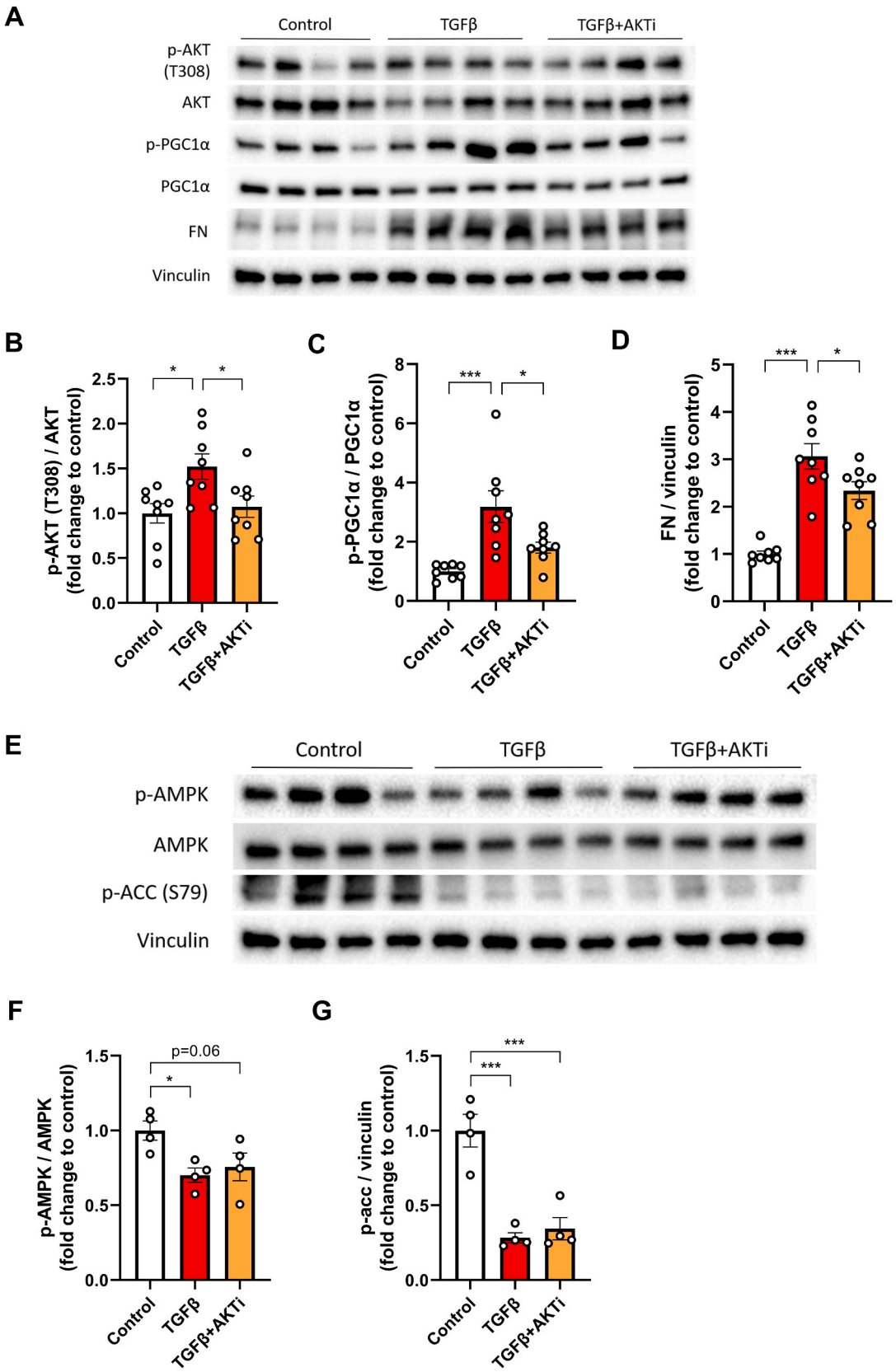

Fig. 8. Inhibiting AKT signaling preserves TGFβ-induced fibrotic changes in HK-2 cells. An AKT inhibitor was added to the HK-2 cells together with TGFβ induction for 48 h. Related protein expression was evaluated and quantified (A–G). Data are presented as mean ± SEM. *P < 0.05, ***P < 0.001 between indicated groups.

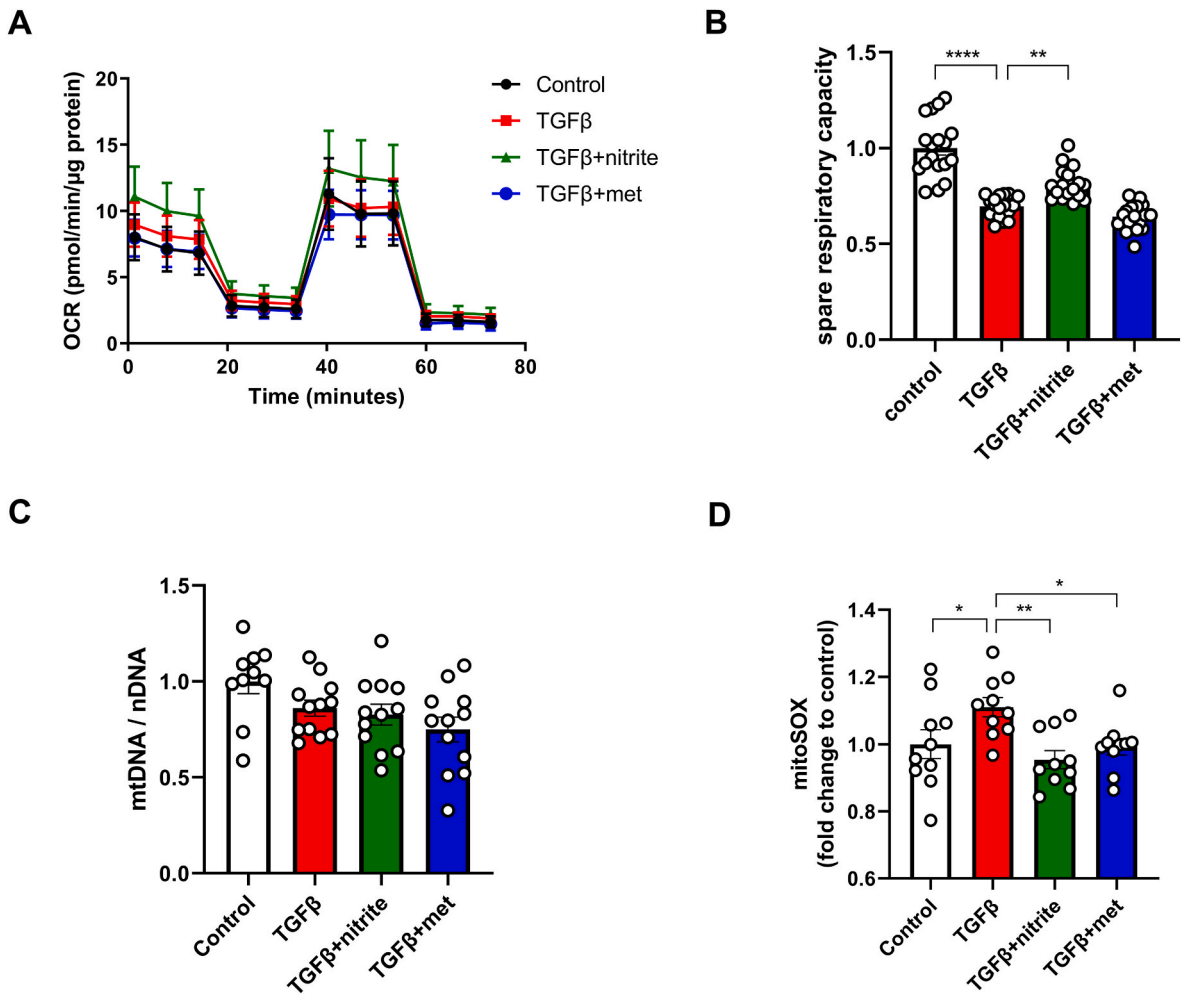

Fig. 9. Nitrite improves TGFβ-mediated mitochondrial dysfunction. HK-2 cells were treated with TGFβ for 48 h, with or without sodium nitrite or metformin treatment. Mitochondrial respiration was evaluated by Seahorse Mito Stress test, presented by monitored oxygen consumption rate (A), and spare respiratory capacity (B). Mitochondrial density was evaluated by mtDNA/nDNA ratio using qPCR (C). Mitochondrial superoxide production was measured using mitoSOX assay (D). Data are presented as mean ± SEM.

These effects were ameliorated by nitrite *in vitro*. The inhibitory effect on PGC1α phosphorylation by AKT was first discovered in the liver [16], and in this study we report for the first time that AKT-mediated PGC1α inactivation in the kidney contributes to pathophysiological mechanisms in UUO-induced fibrosis. When using an AKT inhibitor, we found that it had similar protective effects on TGFβ-induced fibrosis as those observed with nitrite. Previous studies have demonstrated that oxidative stress can activate the PI3K/AKT pathway in various pathological circumstances [27,28], and metformin might therefore inhibit AKT by ameliorating oxidative stress. Taken together, our results indicate activation of a TGFβ-AKT-PGC1α pathway during fibrosis development in renal tubular cells, which seems independent of AMPK signaling.

The use of HK2 cells is controversial and has been debated. Here we used these cells to complement our *in vivo* data in order to gain some more mechanistic insight. As mentioned in a study by Khundmiri et al., widely used proximal tubular cell lines including HK2 and NRK52E cells do not exhibit high transcriptomic similarity with native proximal tubules, such as lack of CPT1α expression, yet they can still be suitable for certain studies [29]. In the Seahorse assay performed in our study, CPT1-specific inhibitor etomoxir was administrated in the middle of the process, which was accompanied with significant drop in oxygen consumption rate (OCR), indicating decreased mitochondria function. Therefore, CPT1α might still function in HK2 cells in spite of relatively low transcriptomic expression.

In this study, metformin administration (used as a positive control) in UUO mice and in TGFβ-exposed tubular epithelial cells was associated with strong AMPK activation and anti-fibrotic effects. This finding agrees with a previous report demonstrating that metformin protected against both folic acid- and UUO-induced kidney fibrosis by activating AMPK-mediated ACC phosphorylation [6]. Metformin also dampened oxidative stress by inhibiting NADPH oxidase activity, as well as mitochondria-specific superoxide production, which should increase the efficiency of oxidative phosphorylation in the mitochondria. However, the Seahorse data showed reduced respiration following administration of metformin. This result was similar to a previous finding using metformin in cancer cells and isolated mitochondria [30]. Although further mechanistic studies are required, stronger activation of AMPK signaling by metformin might explain the difference in mitochondria respiration from that of nitrite.

The reduction of nitrate-to-nitrite is dependent on commensal bacteria in the mouth whereas the conversion of nitrite to bioactive nitrogen species including NO during normoxia in bacteria-independent and may occur both non-enzymatically (*e.g.* at low pH) and enzymatically (*e.g.* by deoxyhaemoglobin, deoxymyoglobin, xanthine oxidoreductase, mitochondrial complexes and by NOS) [8–11]. Meanwhile, hypoxia is another key factor to stimulate NO formation and signaling from inorganic nitrite. We found that HK2 cells exposed to 2 h of hypoxia followed by 24 h of reoxygenation had significant lower viability, which could be

largely prevented by nitrite (*data not shown*). It would be of interest to further investigate and compare the metabolic effects of nitrite with and without hypoxic conditions. To what extent regional hypoxia or lowering of oxygen tension occurs in the obstructed kidney (*in vivo*) or intracellularly in HK-2 cells (*in vitro*) is not clear from the current study, and requires further investigation.

5. Conclusions and future perspectives

Dietary nitrate treatment attenuates the development of kidney fibrosis in a mouse unilateral ureteral obstruction model, which is accompanied by beneficial effects on associated kidney inflammation and oxidative stress along with restoration of AMPK signaling. Moreover, a novel TGFβ-AKT-PGC1α-mediated pathogenic fibrosis pathway in tubular epithelial cells was discovered, and this could be inhibited by inorganic nitrite treatment. From a clinical perspective, future studies will reveal the therapeutic value of oral inorganic nitrate treatment in order to slow down the development and progression of fibrosis in patients with kidney disease.

Author contributions

X.L. and M.C. designed the study; X.L., Z.Z., L.C., R.L., T.A.S. and H. H. carried out experiments; X.L., Z.Z., L.C., R.L. and M.C. analyzed the data; X.L., Z.Z., L.C. and R.L. made the figures; X.L., S.L., V.A.B., E.W., J. O.L. and M.C. drafted and revised the paper; all authors approved the final version of the manuscript.

Declaration of competing interest

Jon O. Lundberg and Eddie Weitzberg are co-inventors on patent applications related to the therapeutic use of inorganic nitrate and nitrite. The other authors have no conflicts of interest.

Acknowledgement

We thank Carina Nihlén, Annika Olsson and Duarte Ferreira (Karolinska Institutet, Stockholm, Sweden) for their technical assistance. This work was supported by grants from the National Natural Science Foundation of China (81600546), CAMS Innovation Fund for Medical Sciences (2021-I2M-1-030), the Karolinska Institutet-China Scholarship Council (CSC) programme (ID #201808110158), and grants from the Swedish Research Council (2020-01645, 2016-01381 and 2016-00785), the Swedish Heart and Lung Foundation (20140448, 20170124 & 20210431), NovoNordisk (2019#0055026), and by EFSD/Lilly European Diabetes Research Programme (2018#97012), as well as Research Funds (2–560/2015) and KID funding (2–3707/2013 & 2–1930/2016) from the Karolinska Institutet, Stockholm, Sweden.

Appendix A. Supplementary data

Supplementary data to this article can be found online at https://doi.org/10.1016/j.redox.2022.102266.

References

[1] A. Djamali, Oxidative stress as a common pathway to chronic tubulointerstitial injury in kidney allografts, Am. J. Physiol. Ren. Physiol. 293 (2007).
[2] L.M. Black, J.M. Lever, A. Agarwal, Renal inflammation and fibrosis: a double-edged sword, J. Histochem. Cytochem. 67 (2019) 663–681.
[3] D. Zhou, Y. Liu, Renal fibrosis in 2015: understanding the mechanisms of kidney fibrosis, Nat. Rev. Nephrol. 12 (2016) 68–70.
[4] A.J. Clark, S.M. Parikh, Targeting energy pathways in kidney disease: the roles of Sirtuins, AMPK, and PGC1alpha, Kidney Int. (2020).
[5] H.M. Kang, S.H. Ahn, P. Choi, Y.A. Ko, S.H. Han, F. Chinga, A.S. Park, J. Tao, K. Sharma, J. Pullman, E.P. Bottinger, I.J. Goldberg, K. Susztak, Defective fatty acid oxidation in renal tubular epithelial cells has a key role in kidney fibrosis development, Nat. Med. 21 (2015) 37–46.
[6] M. Lee, M. Katerelos, K. Gleich, S. Galic, B.E. Kemp, P.F. Mount, D.A. Power, Phosphorylation of Acetyl-CoA carboxylase by AMPK reduces renal fibrosis and is essential for the anti-fibrotic effect of metformin, J. Am. Soc. Nephrol. 29 (2018) 2326–2336.
[7] M.L. Sundqvist, F.J. Larsen, M. Carlstrom, M. Bottai, J. Pernow, M.L. Hellenius, E. Weitzberg, J.O. Lundberg, A randomized clinical trial of the effects of leafy green vegetables and inorganic nitrate on blood pressure, Am. J. Clin. Nutr. 111 (2020) 749–756.
[8] J.O. Lundberg, E. Weitzberg, M.T. Gladwin, The nitrate-nitrite-nitric oxide pathway in physiology and therapeutics, Nat. Rev. Drug Discov. 7 (2008) 156–167.
[9] M. Carlstrom, M.F. Montenegro, Therapeutic value of stimulating the nitrate-nitrite-nitric oxide pathway to attenuate oxidative stress and restore nitric oxide bioavailability in cardiorenal disease, J. Intern. Med. 285 (2019) 2–18.
[10] J.O. Lundberg, M. Carlstrom, F.J. Larsen, E. Weitzberg, Roles of dietary inorganic nitrate in cardiovascular health and disease, Cardiovasc. Res. 89 (2011) 525–532.
[11] M. Carlstrom, Nitric oxide signalling in kidney regulation and cardiometabolic health, Nat. Rev. Nephrol. 17 (2021) 575–590.
[12] I. Cordero-Herrera, M. Kozyra, Z. Zhuge, S. McCann Haworth, C. Moretti, M. Peleli, M. Caldeira-Dias, A. Jahandideh, H. Huirong, J.C. Cruz, A.L. Kleschyov, M. F. Montenegro, M. Ingelman-Sundberg, E. Weitzberg, J.O. Lundberg, M. Carlstrom, AMP-activated protein kinase activation and NADPH oxidase inhibition by inorganic nitrate and nitrite prevent liver steatosis, Proc. Natl. Acad. Sci. U. S. A. 116 (2019) 217–226.
[13] H. Kim, S.Y. Moon, J.S. Kim, C.H. Baek, M. Kim, J.Y. Min, S.K. Lee, Activation of AMP-activated protein kinase inhibits ER stress and renal fibrosis, Am. J. Physiol. Ren. Physiol. 308 (2015) F226–F236.
[14] Y. Dong, Q. Zhang, J. Wen, T. Chen, L. He, Y. Wang, J. Yin, R. Wu, R. Xue, S. Li, Y. Fan, N. Wang, Ischemic duration and frequency determines AKI-to-CKD progression monitored by dynamic changes of tubular biomarkers in IRI mice, Front. Physiol. 10 (2019) 153.
[15] I. Cordero-Herrera, D.D. Guimaraes, C. Moretti, Z. Zhuge, H. Han, S. McCann Haworth, A.E. Uribe Gonzalez, D.C. Andersson, E. Weitzberg, J.O. Lundberg, M. Carlstrom, Head-to-head comparison of inorganic nitrate and metformin in a mouse model of cardiometabolic disease, Nitric Oxide 97 (2020) 48–56.
[16] X. Li, B. Monks, Q. Ge, M.J. Birnbaum, Akt/PKB regulates hepatic metabolism by directly inhibiting PGC-1alpha transcription coactivator, Nature 447 (2007) 1012–1016.
[17] S.M. Houten, S. Violante, F.V. Ventura, R.J. Wanders, The biochemistry and physiology of mitochondrial fatty acid beta-oxidation and its genetic disorders, Annu. Rev. Physiol. 78 (2016) 23–44.
[18] M. Carlstrom, A.E. Persson, E. Larsson, M. Hezel, P.G. Scheffer, T. Teerlink, E. Weitzberg, J.O. Lundberg, Dietary nitrate attenuates oxidative stress, prevents cardiac and renal injuries, and reduces blood pressure in salt-induced hypertension, Cardiovasc. Res. 89 (2011) 574–585.
[19] D.D. Guimaraes, J.C. Cruz, A. Carvalho-Galvao, Z. Zhuge, S.M. Marques, L. M. Naves, A.E.G. Persson, E. Weitzberg, J.O. Lundberg, C.M. Balarini, G.R. Pedrino, V.A. Braga, M. Carlstrom, Dietary nitrate reduces blood pressure in rats with angiotensin II-induced hypertension via mechanisms that involve reduction of sympathetic hyperactivity, Hypertension 73 (2019) 839–848.
[20] A. Ahluwalia, M. Gladwin, G.D. Coleman, N. Hord, G. Howard, D.B. Kim-Shapiro, M. Lajous, F.J. Larsen, D.J. Lefer, L.A. McClure, B.T. Nolan, R. Pluta, A. Schechter, C.Y. Wang, M.H. Ward, J.L. Harman, Dietary nitrate and the epidemiology of cardiovascular disease: report from a National Heart, Lung, and blood institute workshop, J. Am. Heart Assoc. 5 (2016).
[21] M. Hezel, M. Peleli, M. Liu, C. Zollbrecht, B.L. Jensen, A. Checa, A. Giulietti, C. E. Wheelock, J.O. Lundberg, E. Weitzberg, M. Carlstrom, Dietary nitrate improves age-related hypertension and metabolic abnormalities in rats via modulation of angiotensin II receptor signaling and inhibition of superoxide generation, Free Radic. Biol. Med. 99 (2016) 87–98.
[22] C.K.B. L.A. Juncos, A.F. Lopez-Ruiz, L.I. Juncos, Interaction between Stenotic and Contralateral Kidneys: Unique Features of Each in Unilateral Disease. Renal Vascular Disease, Springer, London, 2014.
[23] C. Eisner, R. Faulhaber-Walter, Y. Wang, A. Leelahavanichkul, P.S. Yuen, D. Mizel, R.A. Star, J.P. Briggs, M. Levine, J. Schnermann, Major contribution of tubular secretion to creatinine clearance in mice, Kidney Int. 77 (2010) 519–526.
[24] M.C. Bulbul, T. Dagel, B. Afsar, N.N. Ulusu, M. Kuwabara, A. Covic, M. Kanbay, Disorders of lipid metabolism in chronic kidney disease, Blood Purif. 46 (2018) 144–152.
[25] M. Herman-Edelstein, P. Scherzer, A. Tobar, M. Levi, U. Gafter, Altered renal lipid metabolism and renal lipid accumulation in human diabetic nephropathy, J. Lipid Res. 55 (2014) 561–572.
[26] A.E. Decleves, Z. Zolkipli, J. Satriano, L. Wang, T. Nakayama, M. Rogac, T.P. Le, J. L. Nortier, M.G. Farquhar, R.K. Naviaux, K. Sharma, Regulation of lipid accumulation by AMP-activated kinase [corrected] in high fat diet-induced kidney injury, Kidney Int. 85 (2014) 611–623.
[27] X. Wang, K.D. McCullough, T.F. Franke, N.J. Holbrook, Epidermal growth factor receptor-dependent Akt activation by oxidative stress enhances cell survival, J. Biol. Chem. 275 (2000) 14624–14631.
[28] R. Aikawa, M. Nawano, Y. Gu, H. Katagiri, T. Asano, W. Zhu, R. Nagai, I. Komuro, Insulin prevents cardiomyocytes from oxidative stress-induced apoptosis through activation of PI3 kinase/Akt, Circulation 102 (2000) 2873–2879.
[29] S.J. Khundmiri, L. Chen, E.D. Lederer, C.R. Yang, M.A. Knepper, Transcriptomes of major proximal tubule cell culture models, J. Am. Soc. Nephrol. 32 (2021) 86–97.
[30] S. Andrzejewski, S.P. Gravel, M. Pollak, J. St-Pierre, Metformin directly acts on mitochondria to alter cellular bioenergetics, Cancer Metabol. 2 (2014) 12.